ELSEVIER

0141-1187(95)00008-9

Applied Ocean Research 17 (1995) 155–164

0141-1187/95/$09.50

Hydrodynamic characteristics of an oscillating water column device

D. V. Evans & R. Porter
School of Mathematics, University of Bristol, Bristol BS8 1TW, UK

(Received 20 March 1995; accepted 18 May 1995)

We consider a wave energy device consisting of a thin vertical surface-piercing barrier next to a vertical wall in finite depth water. Power is extracted due to a normally incident wave forcing the free surface of the fluid between the barrier and the wall to oscillate, in turn pumping the volume of air above the free surface through a uni-directional turbine housed at the opening of the device. Under the assumptions of linear water wave theory, the important hydrodynamic properties are expressible in terms of integral quantities of functions proportional to the fluid velocity under the barrier. These functions each satisfy integral equations, the solutions of which are approximated very accurately and efficiently using a Galerkin method as described in Porter and Evans [Porter, R. & Evans, D. V., Complementary approximations to wave scattering by vertical barriers. *J. Fluid Mech.*, **294** (1995) 155–80].

1 INTRODUCTION

Many of the ingenious devices invented to convert the energy of ocean waves into a useful form involve the relative motion of large rigid bodies, the coupling between the bodies being exploited to extract energy. The low frequency of the motion, typically of the order of 10^{-1} Hz provides a challenge to engineers to convert this motion to electrical energy where typically frequencies are of the order of 50 Hz.

One class of device which seeks to avoid this problem, by the use of high-speed air turbines, is the oscillating water column (OWC). The principle of an OWC is simple. Imagine a vertical circular cylindrical tube open at both ends, partly immersed in a narrow wave flume. If the tube is sufficiently narrow, the fluid inside can be regarded as a rigid body when excited by plane waves of given frequency $\omega/2\pi$. Simple hydrostatic arguments then show that the fluid in the tube resonates at a frequency given by $\omega^2 = gl$, where l is the depth of immersion, and a simple experiment does indeed show large internal motions of the fluid in the tube. If the top of the tube is now closed by a cap containing a small hole, the air above the internal free surface will be subject to increased pressure as it tries to escape during the upward motion of the internal fluid surface. By varying the size of the hole, the amount of damping due to viscous losses at the orifice can be altered and energy can be extracted from the incident waves. In practice, the OWC would be quite different. It could be standing on the sea-bed and have a 'mouth', corresponding to the lower opening of the cylindrical tube, whose shape and size is dictated by both efficiency and engineering considerations and the trapped air above the internal free surface would probably be forced through a uni-directional turbine of the Wells type.

In order to provide an input to design considerations, it is important to make some estimate of the hydrodynamic performance of the OWC under typical operating conditions. Early theories for wave-energy devices concentrated on rigid-body models in an attempt to predict performance of devices such as the Salter 'duck', the Cockerell articulated raft or the Bristol submerged cylinder. Thus the work of Evans,[1] Mei,[2] Newman,[3] and Budal and Falnes[4] all provided useful and interesting theoretical results for such problems, both in two and three dimensions. An application of the rigid-body theory to a simple OWC model was provided by Evans.[5] More generally, it was argued that in long waves at least, the internal fluid motion could indeed be regarded as a solid mass with the free surface acting as a light rigid piston. This required the attribution of a value to the 'added mass' of this body of fluid. In 1980, Falcão and Sarmento[6] sought to improve on this model of an OWC by allowing for the increased pressure at the free surface and for the possibility of a non-plane wave surface. This work was generalised by Evans[7] who provided a general theory for any number of fixed rigid bodies each enclosing an internal free surface experiencing an increased pressure. He showed that there was a parallel with the rigid-body motion, provided the ideas of exciting forces on fixed bodies and the given velocities of moving bodies were replaced by the ideas of volume flux across the internal free surfaces open to the atmosphere and the given forcing pressures on those free surfaces, respectively. A further generalisation was provided by Falnes and McIver[8] who, in addition to the internal pressure distribution, also allowed the possibility of motion of the rigid bodies. An application of these ideas to a simple two-dimensional model of an OWC was given by Smith[9] who used the method of matched eigenfunction expansions to solve the boundary-value problems which occur.

There are two reasons why the pressure distribution model is desirable for modelling OWC devices. First is the pedagogical reason that it is simply a more accurate representation of the physical problem since, in experiments, the internal free surface is often observed to be non-plane. Secondly, it is now clear that to model accurately non-linear aspects of the energy conversion, such as the power take-off mechanism, or to apply modern optimal control to the overall system, it is necessary to operate in the time domain rather than the frequency domain. Crucial to such time-domain modelling is a convolution-type integral which represents the 'memory' of the fluid and which contains a kernel function which is essentially a sine or cosine transform of a function in the frequency domain. This function, which on a rigid-body model would just be the added mass or radiation damping, and which in a pressure distribution model is related to the induced volume flux across the internal free surface, needs to be computed accurately at all frequencies from the steady-state frequency-domain problem. Furthermore, in any systematic optimisation procedure involving a variation in geometric and power take-off parameters, it will be important to have an accurate and efficient method for repeated calculation of this function. This is the purpose of the present paper. It is shown how the hydrodynamic characteristics for a simple model of a two-dimensional OWC can be calculated using a Galerkin method. The method has recently been applied to a number of problems in water waves involving vertical barriers in finite depth water (Porter and Evans[10]).

In Section 2, the problem is formulated on the basis of classical linear water-wave theory and the general results needed from the pressure distribution theory are presented. Matched eigenfunction expansions are used to establish integral equations for the volume flux across the free surface from which physical quantities of interest can be determined. The Galerkin method of approximation is described in Section 3 where it is shown how the problem can be reduced to a finite system of algebraic equations, the solution of which yields the elements of a 2×2 real

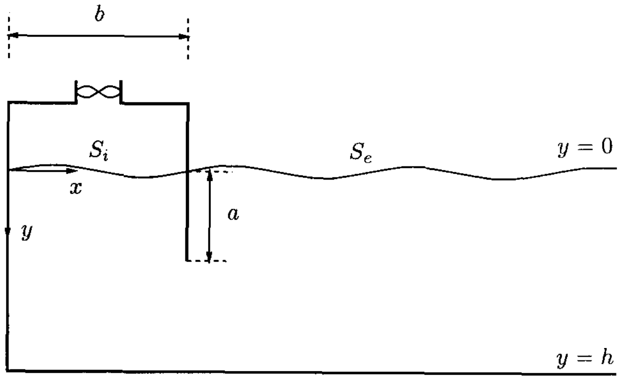

Fig. 1. Definition sketch.

matrix from which all the quantities of interest can be calculated. An added bonus to the method is the fact that the various reciprocity relations which are known to exist between certain hydrodynamical properties of the solution can be proved directly from this matrix formulation. In related problems, authors often use such relations as a check on the accuracy of their numerical computations, although it is frequently the case that such checks appear to be independent of the truncation size. In any event, in the present approach, the relations appear as identities.

The results are described in Section 4 and typical curves of the hydrodynamical coefficients are presented for a range of different parameters. The method turns out to be extremely accurate and efficient computationally and there is no difficulty in extending the results to high frequencies as required for time-domain approaches.

2 FORMULATION

Cartesian co-ordinates are chosen with the mean free surface at $y = 0$. The fluid occupies $0 < y < h$, $0 < x < \infty$ and the water column device consists of a thin vertical surface-piercing barrier of length a, a distance b from a vertical wall which is situated at $x = 0$, as shown in Fig. 1. The volume of air above the internal free surface is connected to the atmosphere via a turbine.

We denote the barrier by $L_b = \{x, y : x = b, 0 \le y \le a\}$ and the gap under the barrier by $L_g = \{x, y : x = b, a < y \le h\}$ and the internal and external free surfaces by $S_i = \{x, y : y = 0, 0 < x < b\}$ and $S_e = \{x, y : y = 0, b < x < \infty\}$ respectively.

Under the usual assumptions of linear water-wave theory, the two-dimensional flow can be expressed in terms of a velocity potential $\Phi(x, y, t)$. Then Φ satisfies

$$\nabla^2 \Phi = 0, \quad \text{in the fluid} \tag{1}$$

$$\Phi_n = 0, \quad \text{on solid boundaries} \tag{2}$$

where the suffix n denotes the normal derivative, whilst the linearised free-surface condition becomes

$$gH - \frac{\partial \Phi}{\partial t} = \begin{cases} P(t)/\rho, & \text{on } S_i \\ 0, & \text{on } S_e \end{cases} \tag{3}$$

where ρ is the density of the fluid and where $H(x, t)$ is the surface elevation and is related to the velocity potential through

$$\frac{\partial H}{\partial t} = \frac{\partial \Phi}{\partial y}, \quad \text{on } y = 0 \tag{4}$$

It is assumed that the motion is time-harmonic with angular frequency ω and so we introduce the time-independent quantities ϕ, p and η by

$$\begin{aligned} \Phi(x, y, t) &= \mathrm{Re}\left\{\phi(x, y)e^{-i\omega t}\right\} \\ P(t) &= \mathrm{Re}\left\{pe^{-i\omega t}\right\} \\ H(x, t) &= \mathrm{Re}\left\{\eta(x)e^{-i\omega t}\right\} \end{aligned} \tag{5}$$

After combining all of the above, the problem can now be expressed in terms of the time-independent velocity potential, ϕ, satisfying the following

$$\nabla^2\phi = 0, \quad \text{in the fluid} \tag{6}$$

$$\phi_y = 0, \quad \text{on } y = h \tag{7}$$

$$\phi_x = 0, \quad \text{on } x = 0 \tag{8}$$

$$\phi_x = 0, \quad (x, y) \in L_b \tag{9}$$

with

$$K\phi + \frac{\partial \phi}{\partial y} = \begin{cases} -i\omega p/\rho g, & \text{on } S_i \\ 0, & \text{on } S_e \end{cases} \tag{10}$$

where $K = \omega^2/g$, and

$$\phi, \ \phi_x \text{ are continuous for } (x, y) \in L_g \tag{11}$$

A suitable radiation condition must also be enforced. Separation of variables allows vertical eigenfunctions to be constructed which are orthonormal over $[0, h]$. They are

$$\psi_n(y) = N_n^{-1/2} \cos k_n(h - y) \tag{12}$$

where

$$N_n = \frac{1}{2}\left(1 + \frac{\sin 2k_n h}{2k_n h}\right), \quad n = 0, 1, 2, \ldots \tag{13}$$

and where the k_n values are the positive roots of

$$K + k_n \tan k_n h = 0, \quad n = 1, 2, \ldots \tag{14}$$

whilst $k_0 = -ik$ and k is the positive root of

$$K = k \tanh kh \tag{15}$$

Then ψ_n values satisfy

$$\frac{1}{h}\int_0^h \psi_n(y)\psi_m(y)\, dy = \delta_{mn} \tag{16}$$

Following the method of Evans,[7] we decompose the potential into two parts such that

$$\phi = \phi^S - \frac{i\omega p}{\rho g}\phi^R \tag{17}$$

where ϕ^S is the solution of the problem of the scattering of a wave incident from $x = +\infty$ in the absence of an imposed pressure on the internal free surface and satisfies eqns (6)–(11) with $p = 0$ in eqn (10). Here, ϕ^R is the solution of the radiation problem defined by eqns (6)–(11) with eqn (10) replaced by

$$K\phi^R + \frac{\partial \phi^R}{\partial y} = \begin{cases} 1, & \text{on } S_i \\ 0, & \text{on } S_e \end{cases} \tag{18}$$

due to an oscillating pressure distribution on S_i in the absence of incoming waves.

Thus, the far-field behaviour of these potentials is of the form

$$\phi^R(x, y) \sim A^R e^{ik(x-b)}\psi_0(y), \quad \text{as } x \to +\infty \tag{19}$$

$$\phi^S(x, y) \sim (e^{-ik(x-b)} + Re^{ik(x-b)})\psi_0(y), \quad \text{as } x \to +\infty \tag{20}$$

where A^R is related to the amplitude of the wave radiated to $+\infty$ due to the forcing on the internal free surface and R is the amplitude of the reflected incident wave in the scattering problem and will have a modulus of unity since all the incident wave energy must be reflected for this problem.

Of considerable interest, in addition to R and A^R, is the induced volume flux across the internal free surface, $Q(t) = \mathrm{Re}\{qe^{-i\omega t}\}$, so that

$$\begin{aligned} q &= \int_{S_i} \frac{\partial \phi}{\partial y}\, dx \\ &= q^S - \frac{i\omega p}{\rho g} q^R \end{aligned} \tag{21}$$

where q^S and q^R are the volume fluxes across S_i in the scattering and radiation problems, respectively, so that

$$q^{S,R} = \int_{S_i} \frac{\partial \phi^{S,R}}{\partial y}\, dx = \int_{L_g} \frac{\partial \phi^{S,R}}{\partial x}\, dy \tag{22}$$

and where the final step uses continuity of flux arguments in the region $0 < y < h$, $0 < x < b$.

Following Evans[7] we make the convenient but arbitrary decomposition of the volume flux due to the radiation potential, thus

$$-\frac{i\omega p}{\rho g} q^R = (\tilde{B} - i\tilde{A})p \tag{23}$$

where $\tilde{A}$ and $\tilde{B}$ are real and directly analogous to the added mass and radiation damping coefficients in a rigid body system. By analogy with electric circuit theory, and following Falnes and McIver,[8] we shall call the complex quantity $\tilde{B} - i\tilde{A}$ the radiation admittance with $\tilde{B}$ the radiation conductance and $\tilde{A}$ the radiation susceptance. Clearly,

$$\tilde{A} = \frac{\omega}{\rho g}\mathrm{Re}\left\{q^{\mathrm{R}}\right\} \tag{24}$$

and

$$\tilde{B} = \frac{\omega}{\rho g}\mathrm{Im}\left\{q^{\mathrm{R}}\right\} \tag{25}$$

With q^{S} and q^{R} defined in this way, along with the form of the far-field behaviour given by eqns (19) and (20), we can find relations that exist between the various quantities so far introduced. See, for example, Evans.[7] Those relations which are relevant here are

$$\tilde{B} = \frac{\omega}{\rho g}Kkh|A^{\mathrm{R}}|^2 \tag{26}$$

and a relation between the radiated amplitude and the induced volume flux in the scattering problem, namely

$$q^{\mathrm{S}} = -2\mathrm{i}KkhA^{\mathrm{R}} \tag{27}$$

It is also possible to derive an expression for the efficiency of the device based on the assumption that there is a linear relation between the volume flux through the turbine and the pressure drop across it. Hence, we assume

$$q = \Lambda p \tag{28}$$

where Λ is a real control parameter, giving rise to the following expression for the maximum efficiency

$$\eta_{\max} = \frac{2\tilde{B}}{\Lambda_{\mathrm{opt}} + \tilde{B}} \tag{29}$$

where

$$\Lambda_{\mathrm{opt}} = (\tilde{B}^2 + \tilde{A}^2)^{1/2} \tag{30}$$

Details of the derivation of the above theory can be found in, for example, Evans[7] or Smith.[9]

2.1 The radiation problem

We write the generalised radiation potential in $0 < x < b$ as

$$\phi^{\mathrm{R}}(x,\ y) = B_0^{\mathrm{R}}\ \cos kx\psi_0(y) + \sum_{n=1}^{\infty} B_n^{\mathrm{R}}\ \cosh k_n x\psi_n(y) + \frac{1}{K} \tag{31}$$

and in $x > b$ as

$$\phi^{\mathrm{R}}(x,\ y) = A^{\mathrm{R}}\mathrm{e}^{\mathrm{i}k(x-b)}\psi_0(y) + \sum_{n=1}^{\infty} A_n^{\mathrm{R}}\mathrm{e}^{-k_n(x-b)}\psi_n(y) \tag{32}$$

such that eqns (6)–(9) are satisfied and where the $1/K$ term in eqn (31) is included to satisfy eqn (18), the free surface condition. The continuity of the potential and velocity across the gap under the barrier and the no-flow condition on the barrier still need to be imposed. Let

$$U^{\mathrm{R}}(y) \equiv \left.\frac{\partial\phi^{\mathrm{R}}}{\partial x}\right|_{x=b} = \mathrm{i}kA^{\mathrm{R}}\psi_0(y) - \sum_{n=1}^{\infty} k_n A_n^{\mathrm{R}}\psi_n(y) \tag{33}$$

$$= -kB_0^{\mathrm{R}}\sin kb\psi_0(y) + \sum_{n=1}^{\infty} k_n B_n^{\mathrm{R}}\ \sinh k_n b\psi_n(y) \tag{34}$$

Using the orthogonality of the ψ_n values, we obtain

$$\mathrm{i}kA^{\mathrm{R}} = -kB_0^{\mathrm{R}}\ \sin kb = \frac{1}{h}\int_{L_{\mathrm{g}}} U^{\mathrm{R}}(y)\psi_0(y)\ \mathrm{d}y = U_0^{\mathrm{R}} \tag{35}$$

$$-k_n A_n^{\mathrm{R}} = k_n B_n^{\mathrm{R}}\ \sinh k_n b = \frac{1}{h}\int_{L_{\mathrm{g}}} U^{\mathrm{R}}(y)\psi_n(y)\ \mathrm{d}y = U_n^{\mathrm{R}} \tag{36}$$

where the fact that $U^{\mathrm{R}}(y) = 0$ and $y = L_{\mathrm{b}}$ has been used, so that

$$U^{\mathrm{R}}(y) = \sum_{n=0}^{\infty} U_n^{\mathrm{R}}\psi_n(y) \tag{37}$$

Let the jump in potential (or pressure) across $x = b$ be defined by $P^{\mathrm{R}}(y) \equiv [\phi]_{x=b}$. Then

$$P^{\mathrm{R}}(y) = (A^{\mathrm{R}} - B_0^{\mathrm{R}}\cos kb)\psi_0(y) + \sum_{n=1}^{\infty}(A_n^{\mathrm{R}} - B_n^{\mathrm{R}}\cosh k_n b)\psi_n(y) - \frac{1}{K}$$
$$= A^{\mathrm{R}}(1 + \mathrm{i}\cot kb)\psi_0(y) - \frac{1}{K} - \sum_{n=1}^{\infty}\frac{U_n^{\mathrm{R}}}{k_n}(1 + \coth k_n b)\psi_n(y) \tag{38}$$

From eqn (11), $P^{\mathrm{R}}(y) = 0$ for $y \in L_{\mathrm{g}}$. Using this and eqn (36) in eqn (38) we obtain

$$\int_{L_{\mathrm{g}}} U^{\mathrm{R}}(t)K(y,\ t)\ \mathrm{d}t = [A^{\mathrm{R}}(1 + \mathrm{i}\ \cot kb)\psi_0(y) - K^{-1}]kh \tag{39}$$

where

$$K(y,\ t) = \sum_{n=1}^{\infty}\frac{k(1 + \coth k_n b)}{k_n}\psi_n(y)\psi_n(t) \tag{40}$$

We now write $U^{\mathrm{R}}(t)$ as the combination of two functions $u_1(t)$ and $u_2(t)$ in the form

$$aU^{\mathrm{R}}(t) = -K^{-1}khu_1(t) + A^{\mathrm{R}}(1 + \mathrm{i}\cot kb)khu_2(t) \tag{41}$$

Hence, if $u_1(t)$ and $u_2(t)$ satisfy

$$\int_{L_{\mathrm{g}}} u_1(t)K(y,\ t)\ \mathrm{d}t = 1, \quad y \in L_{\mathrm{g}} \tag{42}$$

and

$$\int_{L_g} u_2(t)K(y,\ t)\,\mathrm{d}t = \psi_0(y), \quad y \in L_g \tag{43}$$

then $U^{\mathrm{R}}(t)$ defined by eqn (41) will satisfy eqn (39). We write the above as

$$\int_{L_g} u_i(t)K(y,\ t)\,\mathrm{d}t = d_i(y),\ i = 1,\ 2,$$

$$\text{with } d_i(y) = \begin{cases} 1, & i = 1 \\ \psi_0(y), & i = 2 \end{cases} \tag{44}$$

and define the 2×2 matrix $\mathbf{S}$ by

$$S_{ij} = \int_{L_g} u_i(t)d_j(t)\,\mathrm{d}t,\quad i, j = 1,\ 2 \tag{45}$$

Now from eqn (35)

$$\begin{aligned} \mathrm{i}khA^{\mathrm{R}} &= \int_{L_g} U^{\mathrm{R}}(y)\psi_0(y)\,\mathrm{d}y \\ &= -khK^{-1}S_{12} + A^{\mathrm{R}}(\mathrm{i}\ \cot kb + 1)khS_{22} \end{aligned} \tag{46}$$

after use of eqns (41) and (45), yielding

$$A^{\mathrm{R}} = \frac{K^{-1}S_{12}}{(1 + \mathrm{i}\ \cot kb)S_{22} - \mathrm{i}} \tag{47}$$

on rearrangement. Also, from eqn (22)

$$\begin{aligned} q^{\mathrm{R}} &= \int_{L_g} U^{\mathrm{R}}(y)\,\mathrm{d}y \\ &= A^{\mathrm{R}}(1 + \mathrm{i}\ \cot kb)khS_{21} - K^{-1}khS_{11} \end{aligned} \tag{48}$$

where eqns (41) and (45) have been used. Substituting from eqn (47) and simplifying gives

$$q^{\mathrm{R}} = \frac{-K^{-1}kh\,[(1 + \mathrm{i}\ \cot kb)\Delta - \mathrm{i}S_{11}]}{(1 + \mathrm{i}\cot kb)S_{22} - \mathrm{i}} \tag{49}$$

where $\Delta = S_{11}S_{22} - S_{12}S_{21}$.

2.2 The scattering problem

This problem is identical to the symmetric part of another well-documented problem, namely the scattering of waves by two equally submerged barriers in a finite depth and the derivation of the integral equations for this problem is not difficult, the resulting approximations to which can be found in Porter and Evans.[10] The general scattering potential can be written in $0 < x < b$ as

$$\phi^{\mathrm{S}}(x,\ y) = B_0^{\mathrm{S}}\ \cos kx\psi_0(y) + \sum_{n=1}^{\infty} B_n^{\mathrm{S}} \cosh k_n x\psi_n(y) \tag{50}$$

and in $x > b$ as

$$\begin{aligned} \phi^{\mathrm{S}}(x,\ y) &= \left(\mathrm{e}^{-\mathrm{i}k(x-b)} + R\mathrm{e}^{\mathrm{i}k(x-b)}\right)\psi_0(y) \\ &\quad + \sum_{n=1}^{\infty} A_n^{\mathrm{S}}\mathrm{e}^{-k_n(x-b)}\psi_n(y) \end{aligned} \tag{51}$$

whereby all that remains to be satisfied are the conditions on $x = b$. This leads to the following integral equation for the unknown horizontal velocity, $U^{\mathrm{S}}(y)$, across the gap under the barrier

$$\begin{aligned} &\int_{L_g} U^{\mathrm{S}}(t)K(y,\ t)\,\mathrm{d}t \\ &= \left\{(\hat{R} + 1) + \mathrm{i}\cot kb(\hat{R} - 1)\right\} kh\psi_0(y),\ y \in L_g \end{aligned} \tag{52}$$

where $K(y,\ t)$ is defined by eqn (40) and $\hat{R} = R\mathrm{e}^{-2\mathrm{i}kb}$, and so if $u_2(t)$ is the solution of eqn (43), then $U^{\mathrm{S}}(y)$ defined by

$$U^{\mathrm{S}}(y) = \left\{(\hat{R} + 1) + \mathrm{i}\cot kb(\hat{R} - 1)\right\} khu_2(y) \tag{53}$$

will satisfy eqn (52). It can also be shown that

$$\int_{L_g} U^{\mathrm{S}}(y)\psi_0(y)\,\mathrm{d}y = -\mathrm{i}kh(1 - \hat{R}) \tag{54}$$

$$= \left\{(\hat{R} + 1) + \mathrm{i}\cot kb(\hat{R} - 1)\right\} khS_{22} \tag{55}$$

from eqns (53) and (45). Rearranging the above gives

$$\hat{R} = R\mathrm{e}^{-2\mathrm{i}kb} = -\frac{S_{22} - \mathrm{i}(S_{22}\cot kb - 1)}{S_{22} + \mathrm{i}(S_{22}\cot kb - 1)} \tag{56}$$

and clearly $|R| = 1$ as expected. From eqn (22)

$$\begin{aligned} q^{\mathrm{S}} &= \int_{L_g} U^{\mathrm{S}}(y)\,\mathrm{d}y \\ &= \left\{(\hat{R} + 1) + \mathrm{i}\cot kb(\hat{R} - 1)\right\} khS_{21} \end{aligned} \tag{57}$$

using eqns (53) and (45). Substituting eqn (56) into the above gives

$$q^{\mathrm{S}} = \frac{-2\mathrm{i}khS_{21}}{(1 + \mathrm{i}\cot kb)S_{22} - \mathrm{i}} \tag{58}$$

Combining eqns (44) and (45) gives

$$S_{ij} = \int_{L_g}\int_{L_g} u_j(t)K(y,\ t)u_i(y)\,\mathrm{d}t\,\mathrm{d}y = S_{ji} \tag{59}$$

since $K(y,\ t) = K(t,\ y)$ and so the matrix $\mathbf{S}$ is symmetric.

We have shown how the quantities q^{R}, and hence $\tilde{A}$, $\tilde{B}$, q^{S}, A^{R} and R can all be determined in terms of the real 2×2 matrix S_{ij}, $i, j = 1, 2$ with $S_{21} = S_{12}$. In the next section we shall provide an accurate Galerkin approximation to the system eqn (44) from which the S_{ij} values can be determined easily and accurately. However we first show how the various reciprocal relations which exist for these problems can be shown to be satisfied identically. For example, it is a simple matter to verify eqn (27) using eqns

(47) and (58), whilst using eqn (49) in eqn (25) confirms eqn (26) once eqn (47) is used and shows that

$$\tilde{B} = \frac{\omega b}{\rho g} \frac{kh(Kb)^{-1}S_{12}^2}{(\cot kbS_{22} - 1)^2 + S_{22}^2} \tag{60}$$

In a straightforward application of the method of matched eigenfunction expansions which leads to the solution of infinite systems of equations, it is not evident that these relations are satisfied identically. See for example Smith.[9]

3 THE GALERKIN APPROXIMATION

In operator notation, eqns (44) and (45) can be written

$$\mathcal{K}u_i = d_i, \quad i = 1, 2, \quad \text{with} \begin{cases} d_1 = 1 \\ d_2 = \psi_0 \end{cases} \tag{61}$$

and

$$(u_i,\ d_j) = S_{ij} \tag{62}$$

where $(x,\ y)$ denotes the inner product. Once the matrix has been found through a suitable approximation to u_i in eqn (61), all the important properties of the problem are easily obtained. A Galerkin approximation involves expanding the unknowns $u_i(y)$ in a truncated series of test functions with associated unknown coefficients as follows

$$u_i(y) \simeq \tilde{u}_i(y) = \sum_{n=0}^{N} a_n^{(i)} v_n(y), \quad i = 1,\ 2 \tag{63}$$

and inserting into eqn (61) to give

$$\sum_{n=0}^{N} a_n^{(i)} \mathcal{K} v_n = d_i \tag{64}$$

Multiplying through by $v_m(y)$, $m = 0, \ldots, N$ and integrating over L_g gives

$$\sum_{n=0}^{N} a_n^{(i)} (v_m,\ \mathcal{K} v_n) = (v_m,\ d_i), \quad m = 0, \ldots, N \tag{65}$$

or

$$\sum_{n=0}^{N} a_n^{(i)} K_{mn} = L_m^{(i)} \tag{66}$$

where $K_{mn} = (v_m,\ \mathcal{K} v_n)$ and $L_m^{(i)} = (v_m,\ d_i)$. Also the approximation $\tilde{S}_{ij}$ to S_{ij} is

$$\tilde{S}_{ij} = \sum_{n=0}^{N} a_n^{(i)} (v_n,\ d_j) = \sum_{n=0}^{N} a_n^{(i)} L_n^{(j)} \tag{67}$$

Now

$$K_{mn} = (v_m,\ \mathcal{K} v_n) = \int_{L_g} v_m(y) \int_{L_g} K(y,\ t) v_n(t)\, dt\, dy$$

$$= k \sum_{r=1}^{\infty} \frac{(1 + \coth k_r b)}{k_r} \int_{L_g} v_m(y)\psi_r(y)\, dy \int_{L_g} v_n(t)\psi_r(t)\, dt$$

$$= k \sum_{r=1}^{\infty} \frac{(1 + \coth k_r b)}{k_r} F_{mr} F_{nr} \tag{68}$$

where eqn (39) has been used, and $F_{mr} = (v_m,\ \psi_r)$. Note that

$$F_{m0} = (v_m,\ \psi_0) = (v_m,\ d_2) = L_m^{(2)} \tag{69}$$

Choosing $v_m(y)$, as in Porter and Evans' eqn (2.43),[10] to be

$$v_m(y) = \frac{2(-1)^m}{\pi \{(h-a)^2 - (h-y)^2\}^{1/2}} T_{2m}\left(\frac{h-y}{h-a}\right), \quad a < y < h \tag{70}$$

where $T_n(x) = \cos n\theta$, $x = \cos\theta$ is a Chebychev polynomial, gives

$$F_{mr} = N_r^{-1/2} J_{2m}\{k_r(h-a)\} \tag{71}$$

For a detailed discussion of the choice of the test functions, $v_m(y)$, see Porter and Evans.[10] It is sufficient for now to say that the above choice incorporates the expected behaviour of the velocity at the barrier tip and is complete over the expansion interval. From eqn (68) we have

$$K_{mn} = \sum_{r=1}^{\infty} (kN_r k_r)^{-1}(1 + \coth k_r b) J_{2m}\{k_r(h-a)\} \times J_{2n}\{k_r(h-a)\} \tag{72}$$

whilst

$$L_m^{(2)} = F_{m0} = (-1)^m N_0^{-1/2} I_{2m}\{k(h-a)\} \tag{73}$$

and

$$\begin{aligned} L_m^{(1)} &= (v_m,\ 1) \\ &= \int_a^h \frac{2(-1)^m}{\pi\{(h-a)^2 - (h-y)^2\}^{1/2}} T_{2m}\left(\frac{h-y}{h-a}\right) dy \\ &= \frac{2(-1)^m}{\pi} \int_0^1 \frac{T_{2m}(t)}{(1-t^2)^{1/2}}\, dt \\ &= \frac{2(-1)^m}{\pi} \int_0^{\pi/2} \cos 2m\theta\, d\theta \\ &= \delta_{m0} \end{aligned} \tag{74}$$

To summarise, we calculate the entries K_{mn} of the symmetric matrix **K** using eqn (72) and the two right-hand side vectors with entries $L_m^{(i)}$ given by eqns (73) and (74). The solution of this $(N+1) \times (N+1)$ system yields coefficients $a_m^{(i)}$ which when inserted into eqn (67) give $\tilde{S}_{ij}$, the approximation to S_{ij}. Note that the values obtained for $\tilde{S}_{ij}$ are in fact lower bounds to the true values of S_{ij}. This can be shown as follows. Consider S_{ii}, $i = 1, 2$ first. Then multiplication of eqn (65) by $a_m^{(i)}$ and summation over m shows that the Galerkin approximation $u_i(y)$ satisfies

$$(\tilde{u}_i, \mathcal{K}\tilde{u}_i) = (\tilde{u}_i, d_i) = \tilde{S}_{ii} \tag{75}$$

where $\mathcal{K}u_i = d_i$. Now

$$\begin{aligned} S_{ii} - \tilde{S}_{ii} &= (u_i, \mathcal{K}u_i) - (\tilde{u}_i, \mathcal{K}\tilde{u}_i) \\ &= (u_i, \mathcal{K}u_i) - 2(\tilde{u}_i, \mathcal{K}\tilde{u}_i) + (\tilde{u}_i, \mathcal{K}\tilde{u}_i) \\ &= (u_i, \mathcal{K}u_i) - 2(\tilde{u}_i, \mathcal{K}u_i) + (\tilde{u}_i, \mathcal{K}\tilde{u}_i) \\ &= (u_i - \tilde{u}_i, \mathcal{K}(u_i - \tilde{u}_i)) \geq 0 \end{aligned} \tag{76}$$

where the result $(u, \mathcal{K}v) = (\mathcal{K}u, v) = (v, \mathcal{K}u)$ has been used. Thus

$$0 \leq \tilde{S}_{ii} \leq S_{ii} \tag{77}$$

To show that $\tilde{S}_{ij} \leq S_{ij}$, $i \neq j$, we consider the inequality

$$0 \leq (\tilde{u}_{ij}, \mathcal{K}\tilde{u}_{ij}) \leq (u_{ij}, \mathcal{K}u_{ij}) \tag{78}$$

and we now choose $\tilde{u}_{ij} = \tilde{u}_i \pm \tilde{u}_j$ as an approximation to $u_{ij} = u_i \pm u_j$ to give

$$0 \leq (\tilde{u}_i \pm \tilde{u}_j, \mathcal{K}(\tilde{u}_i \pm \tilde{u}_j)) \leq (u_i \pm u_j, \mathcal{K}(u_i \pm u_j)).$$

Expanding both sides and subtracting the two inequalities gives

$$|\tilde{S}_{ij}| \leq |S_{ij}|, \quad i \neq j \tag{79}$$

4 RESULTS

We introduce the non-dimensionalised quantities μ and ν to represent the radiation susceptance and radiation conductance coefficients through

$$\mu = \frac{\rho g}{\omega b}\tilde{A} \tag{80}$$

and

$$\nu = \frac{\rho g}{\omega b}\tilde{B} \tag{81}$$

The efficiency, $\eta_{\max}$, is then given by

$$\eta_{\max} = \frac{2\nu}{(\nu^2 + \mu^2)^{1/2} + \nu} \tag{82}$$

from eqns (29) and (30).

One of the quantities of interest, $|q^S|$, is non-dimensionalised by the volume flux across the internal free surface of a mass of fluid oscillating as a solid body with amplitude and frequency of the incident wave, $|q^I|$, say, giving rise to

$$\frac{|q^S|}{|q^I|} = \frac{N_0^{1/2}|q^S|}{kb \sinh kh} \tag{83}$$

where q^S is defined by eqn (58).

Table 1. Convergence of the elements of S with increasing N in the case a/h=1/2, b/h=1/8 and Kh=1.55

N	$\tilde{S}_{11}$	$\tilde{S}_{12} = \tilde{S}_{21}$	$\tilde{S}_{22}$
0	0.360999	0.264645	0.194008
1	0.412472	0.319606	0.252694
2	0.414681	0.321857	0.254988
3	0.414719	0.321895	0.255027
4	0.414720	0.321896	0.255027
5	0.414720	0.321896	0.255027

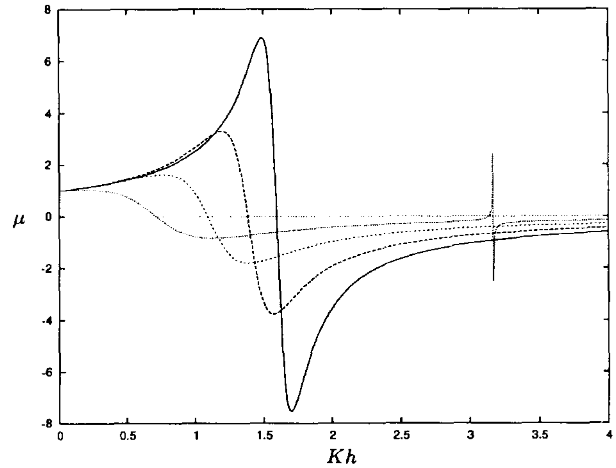

Fig. 2. The radiation susceptance coefficient against Kh in the case of $a/h = 1/2$ for various barrier-to-wall spacings: —— $b/h = \frac{1}{8}$; – – – $b/h = \frac{1}{4}$; - - - - $b/h = \frac{1}{2}$; · · · · · · $b/h = 1$.

It is noted that the K_{mn} values given by eqn (72) require the evaluation of an infinite sum. This is done numerically by truncating the series at a value of M, say. The asymptotic form of the series is used to approximate the remainder as in Porter and Evans[10] in order to provide increased accuracy.

Table 1 illustrates the rapid convergence of the method for a set of parameters Kh, a/h and b/h. The series was truncated at $M = 1500$. It can be seen that convergence is extremely rapid, the elements $\tilde{S}_{ij}$ approaching S_{ij} from below with six-figure accuracy for N as low as 4. Different sets of parameters give equally satisfactory results although larger values of M and N are needed when a/h is very small.

In the graphs which follow, truncation parameters of $N = 4$ and $M = 500$ give at least five-figure accuracy in all cases. Figures 2–5 are all for the case of a fixed barrier-to-depth ratio of $a/h = 1/2$, and barrier-to-back-wall spacing, b/h, varying from 1/8 to 1, whilst Figures 6–9 are all for a fixed barrier-to-back-wall spacing of $b/h = 1$ and barrier-to-depth ratios a/h varying from 1/8 to 3/4. The figures show how μ, ν, $|q^S|$, θ_{q^S} (the phase of q^S) and $\eta_{\max}$ computed from eqn (82) all vary with dimensionless frequency Kh.

There are two situations in which large motions can arise inside the OWC. The more dominant of these, and therefore the one we are more interested in capturing in

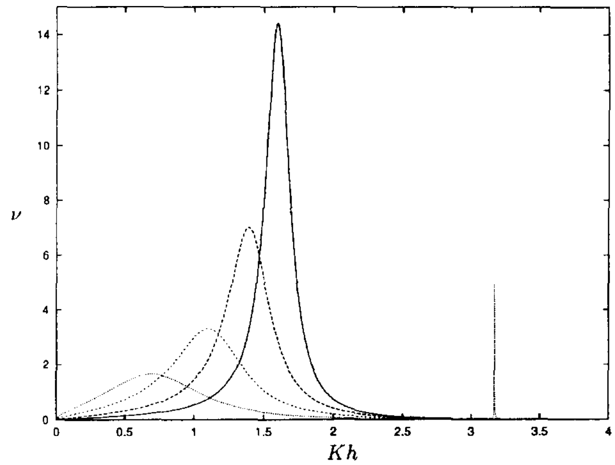

Fig. 3. The radiation conductance coefficient against Kh in the case of $a/h = 1/2$ for various barrier to wall spacings: —— $b/h = \frac{1}{8}$; – – – $b/h = \frac{1}{4}$; - - - - $b/h = \frac{1}{2}$; · · · · · · $b/h = 1$.

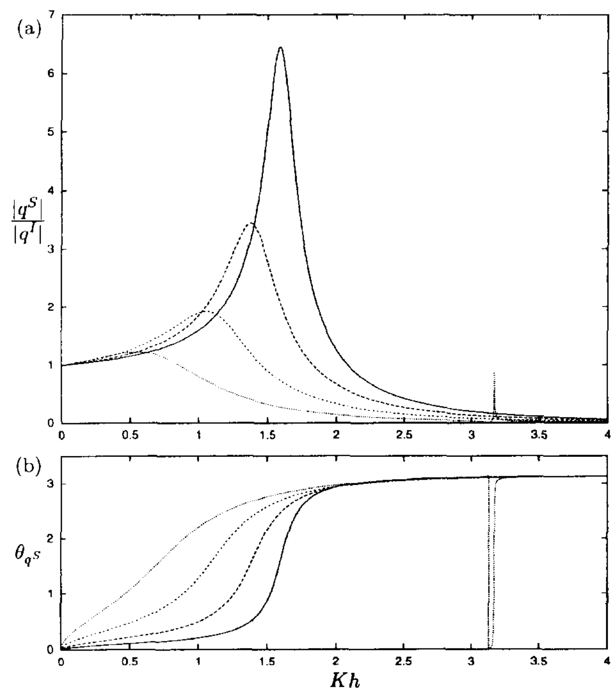

Fig. 4. (a) the magnitude, and (b) the phase of the induced volume flux due to the scattering potential against Kh in the case $a/h = 1/2$ for various barrier to wall spacings: —— $b/h = \frac{1}{8}$; – – – $b/h = \frac{1}{4}$; - - - - $b/h = \frac{1}{2}$; · · · · · · $b/h = 1$.

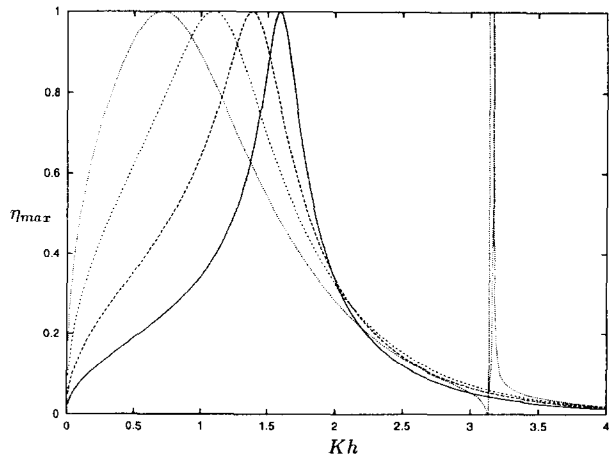

Fig. 5. Efficiency against Kh in the case of $a/h = 1/2$ for various barrier to wall spacings: —— $b/h = \frac{1}{8}$; – – – $b/h = \frac{1}{4}$; - - - - $b/h = \frac{1}{2}$; · · · · · · $b/h = 1$.

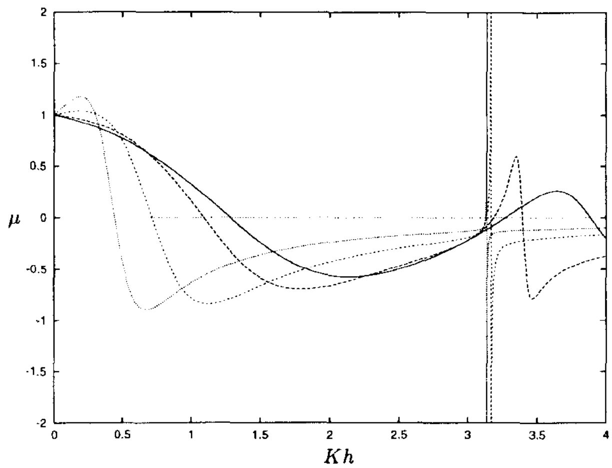

Fig. 6. The radiation susceptance coefficient against Kh in the case of $b/h = 1$ for various barrier submergence depths: —— $a/h = \frac{1}{8}$; – – – $a/h = \frac{1}{4}$; - - - - $a/h = \frac{1}{2}$; · · · · · · $a/h = \frac{3}{4}$.

terms of wave energy, occurs when the fluid between the barrier and the back wall is excited by the incident wave into a resonant piston-like motion inside the OWC. An approximation to this natural frequency of oscillation can be obtained under the assumption that b/a is small and so the fluid in between the walls can be regarded as a solid body. Simple hydrostatic modelling of this situation gives rise to the condition $Ka \approx 1$ for resonance. Thus it can be seen from Fig. 3 that the expected resonance at $Kh = 2$, corresponding to $Ka = 1$, is approached for smaller values of b/h, whilst the effect of a larger spacing is to decrease the frequency at which this resonance occurs, which is explained physically as follows. Increasing the width of the device, b/h, increases the distance a typical fluid particle must travel during a period of motion, a result which can also be obtained by increasing the depth of immersion of the barrier. This argument leads directly to a decrease in the value of Kh at which resonance occurs and since clearly an increase in b/h allows more local fluid motion inside the OWC and thus a breakdown in the solid-body model of resonance, the amplitude of oscillation is decreased.

Large motions inside the OWC can also occur when the incident wave frequency is such that the fluid is excited into an antisymmetric sloshing mode, as though it were in a closed tank with parallel sides. Such a resonance will become more prominent the further the barrier is sub-

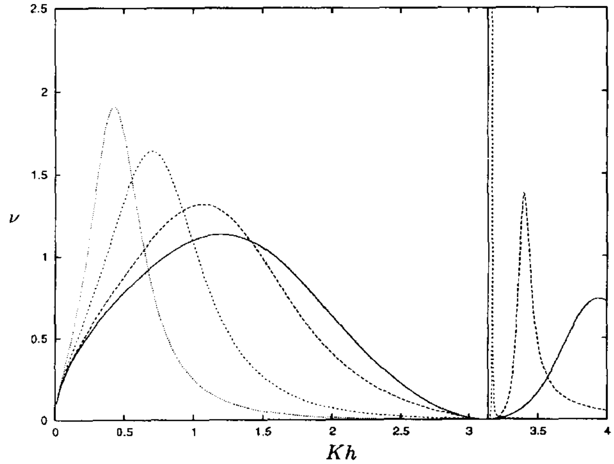

Fig. 7. The radiation conductance coefficient against Kh in the case of $b/h = 1$ for various barrier submergence depths: —— $a/h = \frac{1}{8}$; – – – $a/h = \frac{1}{4}$; - - - - $a/h = \frac{1}{2}$; · · · · · · $a/h = \frac{3}{4}$.

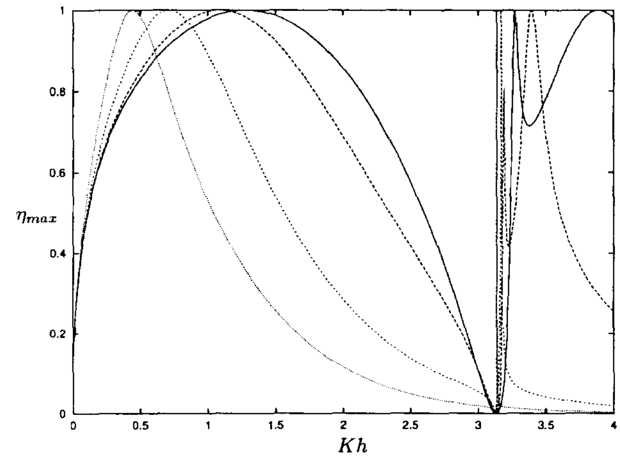

Fig. 9. Efficiency against Kh in the case of $b/h = 1$ for various barrier submergence depths: —— $a/h = \frac{1}{8}$; – – – $a/h = \frac{1}{4}$; - - - - $a/h = \frac{1}{2}$; · · · · · · $a/h = \frac{3}{4}$.

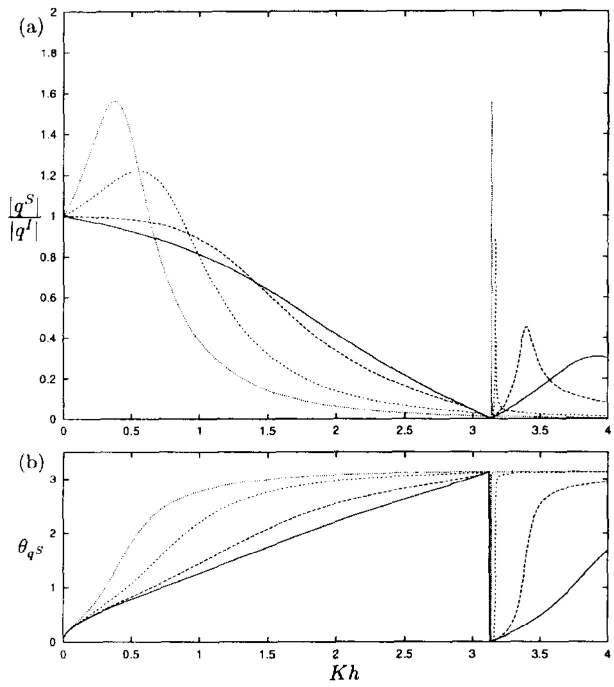

Fig. 8. (a) the magnitude and (b) the phase of the induced volume flux due to the scattering potential against Kh in the case of $b/h = 1$ for various barrier submergence depths: —— $a/h = \frac{1}{8}$; – – – $a/h = \frac{1}{4}$; - - - - $a/h = \frac{1}{2}$; · · · · · · $a/h = \frac{3}{4}$.

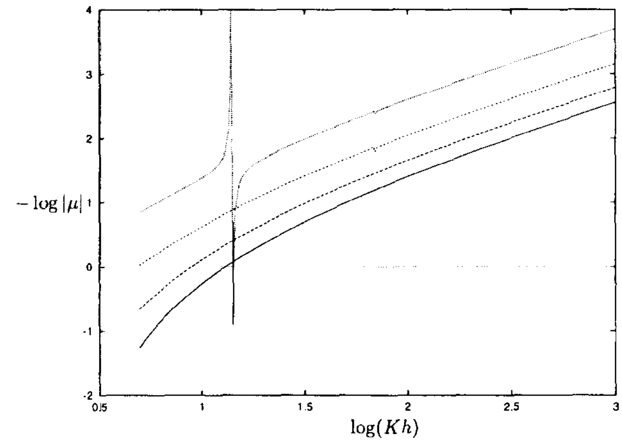

Fig. 10. Asymptotic behaviour of μ, the radiation susceptance, as $Kh \to \infty$, corresponding to the curves in Fig. 2.

merged. In a closed tank, it is straightforward to show that the sloshing frequencies occur at values of the dimensionless wavenumber $kb = n\pi$ and this explains the spiky behaviour in Figs 2–5 for the curve corresponding to $b/h = 1$, the first sloshing mode occuring at $Kh \approx \pi$ in this case. For larger values of Kh, all geometries will give rise to varying degrees of this behaviour and this is shown clearly in Figs 6–9, where b/h is fixed and the depth of submergence of the barrier is allowed to vary. Here, it is seen that for a barrier immersed to only a small proportion of the depth, the resonant effect of the sloshing frequency is small and relatively far away from $kb = \pi$. Increasing the immersion of the barrier moves the resonant frequency nearer to the sloshing frequency in a closed tank, whilst the peak becomes much larger and more spiked.

Associated with every zero of μ is a maximum in $\eta_{\max}$, the maximum efficiency, yielding two peaks in the curves for $\eta_{\max}$ for every resonance where the curve of μ passes through zero twice.

Finally, Fig. 10 shows the behaviour of the radiation susceptance, μ, as $Kh \to \infty$. The knowledge of this asymptotic behaviour is important in the modelling of time-domain approaches and it can be seen from the gradient of the curves in Fig. 10 that $\mu \propto \omega^{-2}$ as $Kh \to \infty$. This is very different from the solid-body equivalent to μ, the so-called added mass, which has been shown to tend to a non-zero constant at high frequencies. The spikes in Fig. 10 are due to resonances at sloshing frequencies.

5 CONCLUSION

An efficient, accurate method has been described for computing the hydrodynamic coefficients associated with a pressure distribution model of a simple OWC device. The method reduces to the solution of a small number of algebraic equations and provides lower bounds to the elements of a 2×2 real matrix which are directly related to all the coefficients of interest. Known reciprocal relations are satisfied identically and the method can be used to obtain accurate values for all frequencies including the large values which are necessary for time-domain modelling of non-linear power take-offs.

ACKNOWLEDGEMENTS

The authors would like to thank Prof. J. Falnes for valuable discussions. R. P. is in receipt of SERC grant No. 92004667.

REFERENCES

1. Evans, D. V., A theory for wave power absorption by oscillating bodies. *J. Fluid Mech.*, **77** (1976) 1–25.
2. Mei, C. C., Power extraction from water waves. *J. Ship. Res.*, **20** (1976) 63–6.
3. Newman, J. N., The interaction of stationary vessels with regular waves. *Proc. 11th Symp. Naval Hydrodynamics*, 1976, pp. 451–501.
4. Budal, K. & Falnes, J., Optimum operation of improved wave-power convertors. *Marine Sciences Comm.*, **3** (1977) 133–50.
5. Evans, D. V., The oscillating water column wave energy device. *J. Inst. Maths Applics*, **22** (1978) 423–33.
6. Falcão, J. & Sarmento, A. J. N. A., Wave generation by a periodic surface pressure and its application in wave-energy extraction. *15th Int. Cong. Theor. Appl. Mech.*, Toronto, 1980.
7. Evans, D. V., Wave-power absorption by systems of oscillating surface pressure distributions. *J. Fluid. Mech.*, **114** (1982) 481–99.
8. Falnes, J. & McIver, P., Surface wave interactions with systems of oscillating bodies and pressure distributions. *Appl. Ocean Res.*, **7** (1985) 225–34.
9. Smith, C. M., Some problems in linear water waves. Ph.D. Thesis, University of Bristol, Bristol, UK, 1983.
10. Porter, R. & Evans, D. V., Complementary approximations to wave scattering by vertical barriers. *J. Fluid Mech.*, **294** (1995) 155–80,